Inorganic Chemistry

Article

pubs.acs.org/IC

Cyclometalated Iridium(III) Imidazole Phenanthroline Complexes as Luminescent and Electrochemiluminescent G-Quadruplex DNA Binders

Katherine J. Castor, Kimberly L. Metera, Ushula M. Tefashe, Christopher J. Serpell, Janine Mauzeroll,* and Hanadi F. Sleiman*

Department of Chemistry, McGill University, 801 Sherbrooke West, Montreal, Quebec H3A 0B8, Canada

Supporting Information

ABSTRACT: Six cyclometalated iridium(III) phenanthroimidazole complexes with different modifications to the imidazole phenanthroline ligand exhibit enhanced luminescence when bound to guanine (G-) quadruplex DNA sequences. The complexes bind with low micromolar affinity to human telomeric and c-myc sequences in a 1:1 complex:quadruplex stoichiometry. Due to the luminescence enhancement upon binding to G-quadruplex DNA, the complexes can be used as selective quadruplex indicators. In addition, the electrogenerated chemiluminescence of all complexes increases in the presence of specific G-quadruplex sequences, demonstrating potential for the development of an ECL-based G-quadruplex assay.

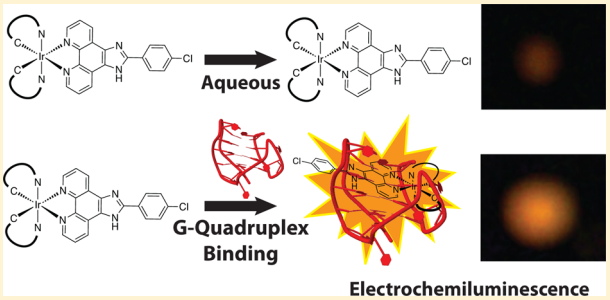

INTRODUCTION

Guanine (G-) quadruplexes are biologically relevant DNA secondary structures formed through hydrogen bonding of guanine units into stacked tetramers. They are localized in specific regions of the genome including telomeres and oncogene promoters. They are particularly interesting targets for detection due to their roles in the development of human cancers.[1−3] G-quadruplex sensing can also aid in the detection of other species, such as nucleic acids, proteins, small molecules, or ions.[4−7] The challenge resides both in the sensitive detection and in the identification of the different G-quadruplex polymorphs that are constituents of these biological processes. In the past two decades, a variety of organic and metal-based complexes have been reported as efficient binders for many G-quadruplex-forming sequences including telomeric DNA, as well as promoter sequences in c-myc, c-kit, and Bcl-2 protooncogenes.[8−10] Square-planar (Pt(II), Pd(II), Ni(II), etc.) and octahedral (Ru(II)) metal-based complexes, such as those reported by us[11−13] and others,[14−18] present a variety of attributes that make them ideal binders, including an inherent positive charge, modular ligand design, and favorable luminescent and electronic properties.

The potential of iridium-based complexes for the binding and detection of biomolecules is becoming increasingly apparent.[19−24] Excellent features of this class of compounds include high quantum yields, long luminescent lifetimes, large Stokes shifts, and tunable emission wavelengths.[25,26] In the past, issues with poor water solubility overshadowed these advantageous characteristics, but more recently iridium complexes have been designed as labels for biomolecules[27,28] and have been used to detect target DNA strands with greater sensitivity than related ruthenium complexes,[29] antibiotics,[30] and enzymes.[31−33]

We describe here a new class of cyclometalated iridium(III) complexes that bind preferentially to G-quadruplex sequences. These synthetically accessible complexes have the general formula $[Ir(ppy)_2(N^N)]^+$, where ppy = 2-phenylpyridinato, and N^N refers to the ancillary ligand based on π-extended phenylimidazole phenanthroline (Scheme 1). The complexes were characterized by absorbance/photoluminescence, electrochemical, and electrochemiluminescence (ECL) measurements, and for complexes **3** and **4**, crystal structure analyses were conducted. The binding affinity of each complex for G-quadruplex sequences 22AG-K and c-myc was also determined. The iridium complexes show a "switch-on" effect, with weak luminescence in water that is significantly enhanced (~50×) in the presence of guanine quadruplexes. Double-stranded or single-stranded DNA does not cause this luminescence enhancement, indicating that the complexes bind preferentially to G-quadruplex DNA. On the basis of these studies, we developed a simple agarose gel electrophoresis staining assay for guanine quadruplexes, in which iridium complexes such as **2** and **4** can distinguish between duplex DNA and G-quadruplexes; this assay also has the potential to distinguish between different G-quadruplex polymorphs found in oncogene promoters and telomeres. Interestingly as well, complexes **2** and **5** exhibit enhanced electrochemiluminescence in the presence of G-quadruplex DNA (human telomeric 22AG-K and

Received: April 28, 2015
Published: June 30, 2015

DOI: 10.1021/acs.inorgchem.5b00921
Inorg. Chem. 2015, 54, 6958−6967

Scheme 1. Synthesis of Complexes 1−7

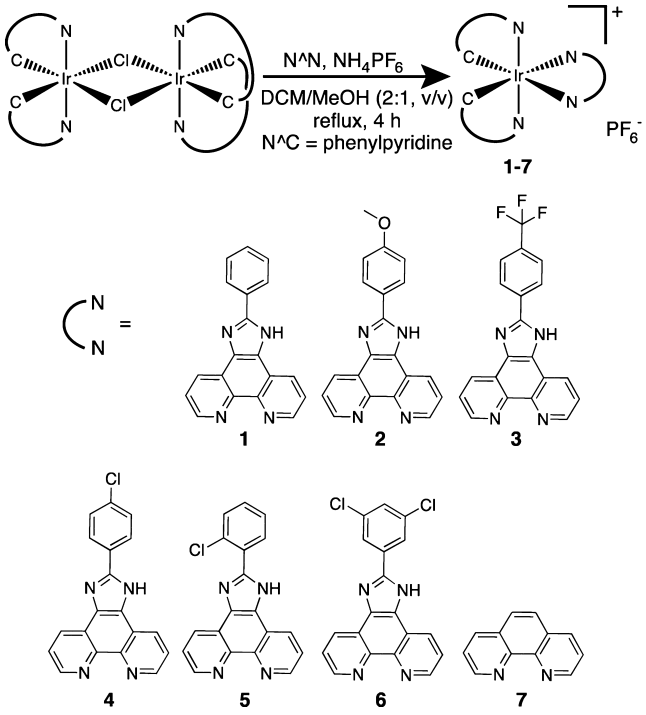

oncogene c-myc), laying the preliminary foundations for a new sensitive and selective detection method. To our knowledge, this is the first report of direct ECL enhancement upon G-quadruplex binding, and this phenomenon is selective for specific G-quadruplex structures.

RESULTS AND DISCUSSION

Crystal Structure Analysis. Single crystals of trifluoromethyl complex **3** and *p*-chloro complex **4** were grown via slow diffusion of acetic acid into a solution of **3** or **4** in dichloromethane. The ORTEP diagram of complex **3** is depicted in Figure 1 (see Supporting Information for details of crystal structure of **3** and specifically at Figure S1 for crystal structure and details of **4**). Interestingly, both molecules **3** and **4** were found to crystallize into a stacked dimer (Figure 1b and Supporting Information Figure S1b). The nitrogen atoms of the phenylpyridinato ligands occupy axial positions on the metal,[34] which results in a cis-C,C trans-N,N chelate configuration. Superimposition of the two molecules in the asymmetric unit revealed that, within a dimer, their stereochemistry was identical (Figure 1c and Supporting Information Figure S1c), while both enantiomers were present in the crystal.

Photophysical Properties. Complexes **1**−**6** were first assessed for their photophysical properties in dichloromethane (DCM) and aqueous environments. From the absorbance data (Table 1 and Supporting Information Figures S2 and S3), for all complexes, intense absorption bands below 320 nm could be observed and are assigned to spin-allowed $\pi-\pi^*$ ligand-centered (LC) transitions for phenylpyridinato and phenanthroline-based ligands.[27,35−40] Moderately intense absorption bands in the range 380-430 nm were also observed that are assigned to spin-allowed metal-to-ligand charge transfer (MLCT) (Ir dπ to phenanthroline π^*), or ligand-to-ligand (LLCT) (ppy π to phenanthroline π^*) transitions (or a combination thereof).[28,35,41] Finally, the weak absorption tails above 430 nm are assigned to spin-forbidden ^{3}MLCT (Ir dπ to phenanthroline π^*) transitions.[27,37]

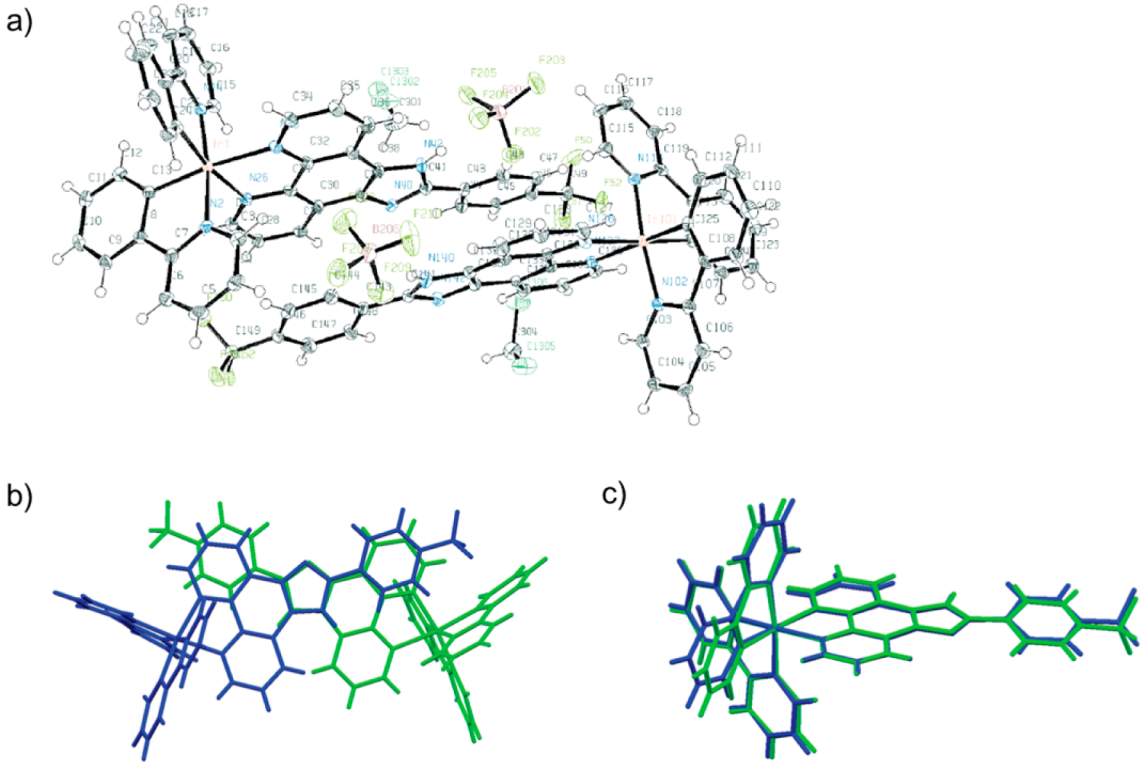

Figure 1. (a) Complete crystal structure of complex **3** showing thermal ellipsoids at 50% probability, (b) dimer of complex **3**, and (c) overlay of two metal complexes in the asymmetric unit, showing their identical stereochemistry.

DOI: 10.1021/acs.inorgchem.5b00921
Inorg. Chem. 2015, 54, 6958−6967

Table 1. Photophysical Properties of complexes 1-6

	λ abs/nm (ε/M^{-1} cm^{-1})		λ_{max} em (nm)		Φ_{em} (%, $Ru(bpy)_3^{2+}$ std)[a]		τ_o (ns)	
	DCM	H_2O	DCM	H_2O	DCM	H_2O	DCM	H_2O[b]
1	282 (52 500), 303 (49 400), 392 (12 000), 472 (2000)	281 (55 200), 308 (46 500), 405 (13 300), 477 (4100)	562	580	3.5	0.43	240	64
2	273 (35 800), 291 (36 400), 412 (6900), 472 (1600)	290 (37 700), 422 (8700), 477 (3500)	565	577	3.4	0.54	213	66
3	272 (45 800), 285 (45 600), 302 (41 100), 393 (9600), 413 (8400), 472 (1300)	284 (41 200), 306 (37 300), 393 (11 400), 415 (8900), 477 (3000)	563	580	3.3	0.89	262	61
4	284 (49 600), 304 (47 200), 394 (11 600), 417 (10 000), 472 (1800)	286 (52 700), 306 (49 900), 396 (16 700), 416 (14 000), 477 (5000)	563	580	3.3	0.16	242	62
5	273 (29 000), 301 (24 100), 389 (6900), 409 (6100), 472 (900)	274 (28 300), 302 (23 200), 398 (7100), 477 (2000)	570	575	3.3	0.98	209	67
6	285 (41 800), 302 (39 000), 391 (10 100), 412 (9000), 472 (1300)	286 (50 500), 304 (47 800), 350 (31 500), 395 (15 600), 477 (4600)	564	580	3.7	0.67	207	57

[a]The Φ of $Ru(bpy_3)^{2+}$ in water is 0.028. [b]The second decay is given as it represents between 89% and 99% of the overall decay. The complete lifetime data for the complexes in water are given in Supporting Information Table S2.

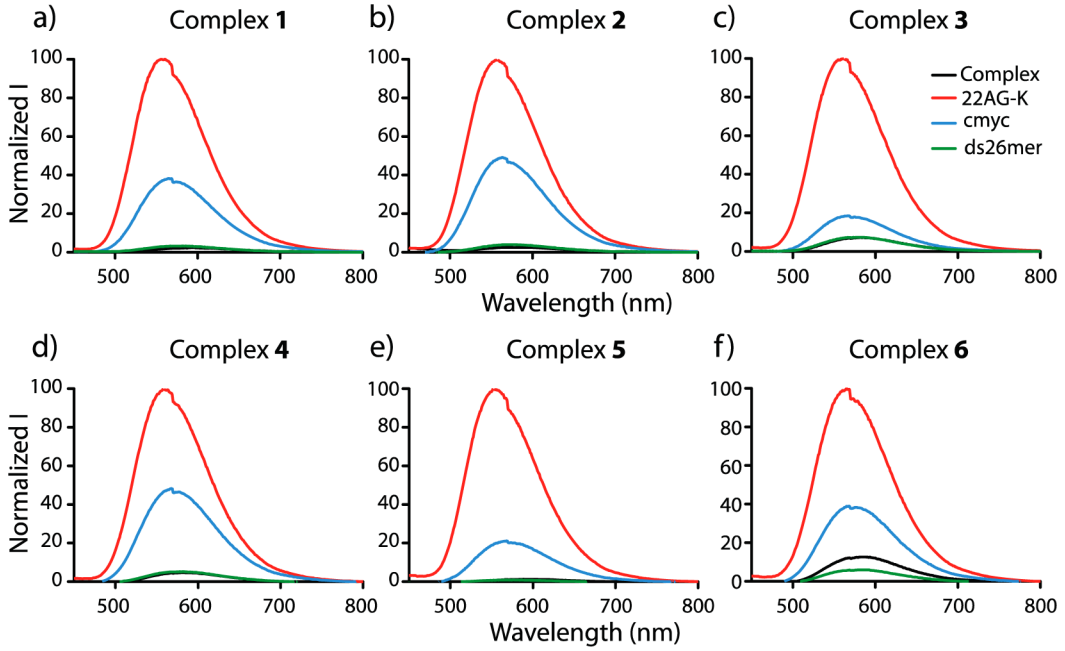

Figure 2. Enhancement of luminescence after incubation in 1×K buffer (10 mM sodium cacodylate with 100 mM KCl, pH 7.2) of the complexes **1**–**6** (2 μM) with excess DNA (20 μM).

The room-temperature photoluminescence data of the complexes in dichloromethane and water are summarized in Table 1, and the spectra are shown in Supporting Information Figures S2 and S3. All complexes emit in the range 579–593 nm with excitation at 280 nm in both DCM and H_2O at room temperature. We can assign the excited-state characteristics of complexes **1**–**6** as mixed MLCT and LLCT transitions. The MLCT results from the promotion of an electron from the HOMO of the metal center (or delocalized between the metal and the ppy, see UV–vis assignment above) to the π^* orbital of the phenanthroline ligand, while the LLCT transition arises from the movement of electrons located on the phenylpyridinato ligands to the phenanthroline π^* orbital.[41−44] The complexes exhibit monoexponential luminescence lifetimes on the order of 207–262 ns in dichloromethane.[45] As a literature comparison, we also assayed complex **7**. Under our experimental conditions, the lifetime of complex **7** is 145 ns, which agrees well with a literature value of ~190 ns.[35]

In aqueous conditions, the quantum yields are significantly reduced. The lifetimes are biexponential with a very rapid decay of 5–9 ns (1–11%), and a longer decay of 57–67 ns (89–99%). The biexponential behavior is consistent with the complexes' poor solubility in aqueous solution, possibly resulting in association, and a two-state decay.[46,47] For comparison, the more water-soluble complex **7** was shown to have a monoexponential lifetime of 92 ns.

Luminescence Enhancement upon Quadruplex Binding. We previously demonstrated that platinum complexes containing imidazole–phenanthroline ligand variations such as that in **1** are excellent binders of guanine quadruplexes and are telomerase inhibitors.[12,13,48] We were thus interested in the binding affinity and selectivity of the iridium complexes **1**–**7** to G-quadruplexes, and whether their photophysical properties were altered upon binding.[49] To this end, we added DNA to the iridium complexes in potassium-containing aqueous buffer, using a 10× excess of DNA to maximize the complex binding. The G-quadruplex-forming DNA strands used were a telomere

DOI: 10.1021/acs.inorgchem.5b00921
Inorg. Chem. 2015, 54, 6958–6967

repeat sequence (22AG-K), an oncogene promoter sequence (c-myc), as well as duplex (dsDNA) and single-stranded (ssDNA) short sequences as controls. The complete sequences of all G-quadruplex polymorphs, duplex, and single-stranded DNA used in this study are in Supporting Information Table S1. The fluorescence results collected after incubation for 1 h at room temperature are shown in Figure 2 and Table 2 (data for ssDNA are shown in Supporting Information Figure S4). All complexes exhibited blue-shifted emission upon DNA binding, likely a result of the nonpolar environment surrounding the G-quadruplex-bound complexes. The charged excited state of the bound complex is not as stabilized by the surrounding medium as for the unbound species by aqueous solvent. Excitingly, all complexes **1**−**6** show much higher emission intensities when bound to G-quadruplex. Binding of complexes **1**−**6** to G-quadruplexes places the complexes in an environment that is relatively solvent inaccessible, thus restoring their luminescence to values closer to those in organic solvent.[15,49−52] The greatest enhancement (53×) was observed for the interaction of complex **5** with telomeric 22AG-K, and this was accompanied by the largest shift in emission maximum (a 42 nm blue-shift). This "light-switch" effect was not observed with duplex or ssDNA. In contrast, the luminescence of complex **7** decreased in the presence of any added DNA (Supporting Information Figure S5), as did the emission of **1**−**6** with added ssDNA (Supporting Information Figure S4). This result was surprising, but is possibly explained upon consideration of the various possible binding modes of complexes to DNA. Besides intercalation, electrostatic interactions and groove binding are also available. Some ruthenium complexes related to complex **7** are known to be (minor) groove binders rather than intercalators.[53,54] It is possible that nonspecific binding to DNA causes association of these complexes on the DNA strands, and results in self-quenching for some of these molecules. This phenomenon is currently being examined in greater detail.

Table 2. Quantification of Luminescence Enhancement and Blue-Shift as a Result of DNA Interaction

		22AG-K		c-myc		ds26mer	
	1×K buffer λ(max)	λ(max)	I_{bound}/I_o	λ(max)	I_{bound}/I_o	λ(max)	I_{bound}/I_o
1	593	557	38.1	566	15.0	582	1.42
2	588	558	27.8	565	14.0	578	1.17
3	584	560	13.0	564	2.45	587	1.05
4	585	559	18.5	564	9.20	579	1.10
5	595	553	52.9	570	11.7	578	0.745
6	583	566	7.3	570	2.92	579	0.493
7	592	568	0.309	562	0.399	588	0.637

While complex emission was enhanced in G-quadruplex versus in dsDNA, showing specificity toward G-quadruplex DNA, enhancements were much more pronounced in telomeric 22AG-K compared to c-myc. This behavior may be attributed to the differences in the folded structures of these polymorphs and the available binding pockets for complexes **1**−**6**. Figure 3 shows one of the possible polymorphs for each of 22AG-K and c-myc, illustrating differences in the placement and rigidity of the loops above and below the surface of the tetrads.[55,56] These loops may be able to shield the iridium complex from the solvent to different extents for these two structures, if the imidazole−phenanthroline ligand inserts between them and the G-tetrad.[15] In general, the end-stacking mode has been shown to be the dominant binding site for these G-quadruplex structures.[57] We verified by circular dichroism that binding of complexes **1** and **7** to both G-quadruplex polymorphs does not significantly affect their structure (Supporting Information Figure S6).

Assessing Binding Affinity and Stoichiometry. After assessing the luminescence enhancement when the complexes bind to G-quadruplex DNA, we devised a direct luminescence assay to study the binding affinity of the library with the biologically relevant G-quadruplex polymorphs telomeric (22AG-K) and c-myc.[59−64] The curves were fit to a one-site binding model in GraphPad Prism, resulting in K_D (dissociation constant) values that are represented in Table 3 (see Supporting Information Figure S7 for the fitted curves). All the complexes show binding affinity in the submicromolar range, which indicates tight binding to the quadruplex sequences examined. Among these samples, the lowest value determined is 0.089 ± 0.031 μM for complex **1** with the c-myc polymorph.

Due to the lack of significant fluorescence enhancement when the complexes bind to duplex DNA, binding affinities to duplex motifs could not be assessed using the direct luminescence enhancement method. Instead, we performed CD melting experiments to determine the extent to which the iridium complexes could thermally stabilize duplex DNA. These results show essentially no thermal stabilization imparted by

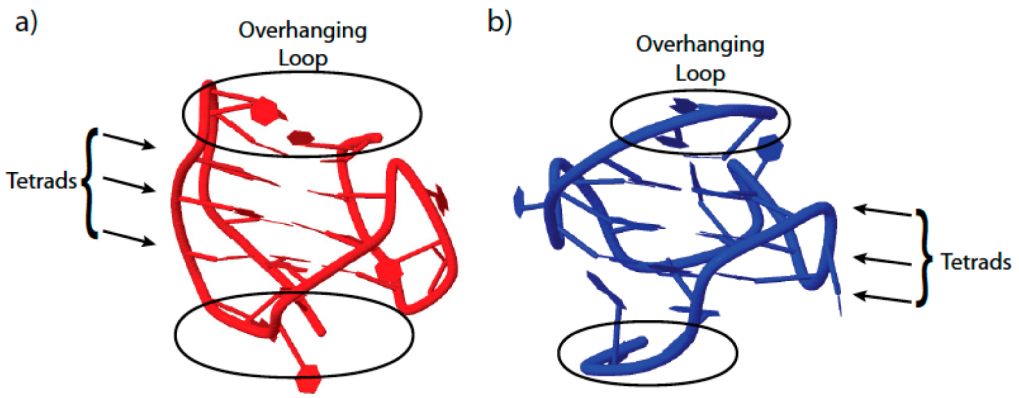

Figure 3. Visual inspection of one of the possible solution structures of (a) 22AG-K and (b) c-myc (Pu-27)[58] (PDB codes 2GKU[55] and 1XAV,[56] respectively). Each structure is shown with the wide groove in the foreground. Tetrads are indicated with arrows while loops are indicated by ellipses.

DOI: 10.1021/acs.inorgchem.5b00921
Inorg. Chem. 2015, 54, 6958−6967

Table 3. Binding Affinity [K_D (μM)] As Determined from the Direct Luminescence Assay

	1	2	3	4	5	6
22AG-K	0.77 ± 0.01	0.22 ± 0.03	0.75 ± 0.14	0.84 ± 0.02	0.21 ± 0.02	0.70 ± 0.10
c-myc	0.089 ± 0.031	0.98 ± 0.02	0.66 ± 0.06	0.85 ± 0.12	1.1 ± 0.5	1.7 ± 0.4

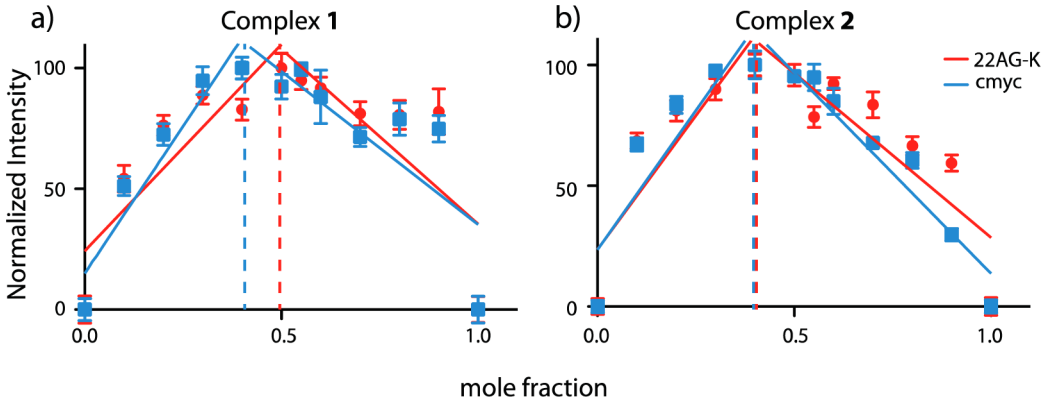

Figure 4. Job plots indicating binding stoichiometry. The error bars represent the standard deviation from duplicate measurements.

representative complex **1** on the DNA duplexes (Supporting Information Figure S8), consistent with the high selectivity of **1**−**6** for G-quadruplex DNA.[65]

To assess the binding stoichiometry of complexes **1**−**6**, a continuous variation method (Job plot) was conducted for binding to 22AG-K and c-myc G-quadruplexes. In this assay, the total concentration of DNA and complex are held constant (10 μM) while the mole fractions of the two components are varied, and each fraction is quantified by luminescence intensity. Complexes **1** and **2** gave the clearest results and are shown in Figure 4, although the results could be expected to be similar for the other complexes as well. The inflection point occurs at ∼0.50 mole fraction, which corresponds to a 1:1 binding stoichiometry, that is, one complex per quadruplex.[66]

Selective G-Quadruplex Dyes for Electrophoresis. An interesting application of the selectivity of the complexes toward G-quadruplexes may be as selective stains for gel electrophoresis in visual, qualitative assays. To this end, we ran duplex and single-stranded DNA along with eight different G-quadruplex forming sequences, including telomeric (22AG-K) and various oncogene sequences (c-myc, ckit1, ckit2, KRAS, BCL2, PDGFA, and VEGF [Supporting Information Table S1)], at 10 μM in structure per lane on a 2% (w/v) native agarose gel (1×TBE-KCl) containing 1.0 μM iridium complexes **1**−**6**. We compared the staining capability of these complexes to the commercially available nucleic acid stain SYBR gold. The intensity graphs from the gel staining for **2** and **4**, the brightest and most selective for G-quadruplex sequences, are compared to SYBR gold in Figure 5. The gels for **2** and **4** are shown in Supporting Information Figure S9, and the intensity graphs for **1**−**5** inclusive are in Supporting Information Figure S10.

As can be ascertained from Figure 5, SYBR gold shows relatively intense staining of double-stranded DNA, and comparatively minimal staining of the G-quadruplexes. In contrast, **2** and **4** show no, or minimal, staining, respectively, of duplex and single-stranded DNA. For some of the complexes, staining is even selective for specific G-quadruplex polymorphs. For example, complex **2** strongly stains the VEGF G-quadruplex structure over the other polymorphs. Complex **4** preferentially stains the c-myc polymorph (the bar graph in

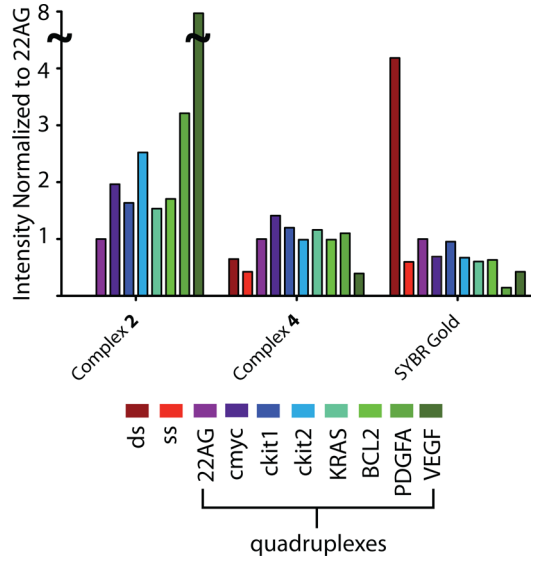

Figure 5. Bar graph depicting the integrated intensities of the bands in the gel staining assay. Gels are shown in Supporting Information Figure S9. For each complex, the intensities are normalized to the intensity of 22AG-K staining.

Figure 5 shows intensities of the complexes that are normalized to the intensity of the 22AG sequence; as such, the intensities cannot be compared across different complexes). The results for the other complexes are shown in Supporting Information Figure S10. Complexes **1**−**5** can be used as selective indicators for G-quadruplexes over double- or single-stranded DNA in gel electrophoresis. Thus, it may be feasible to use complexes **1**−**5** to identify G-quadruplexes from cellular extracts in assays with proper G-quadruplex standards for reliable comparison. In analogy to ethidium bromide methods for duplex DNA, their micromolar binding affinities possibly allow destaining and removal of the complexes, in order to isolate and collect these quadruplexes.[67]

Electrochemistry and ECL. The electrochemical data for complexes **1**−**6** are summarized in Table 4, and cyclic voltammograms (CVs) are shown in Figure 6. In acetonitrile, the CVs are characterized by 2 major redox peaks: a one-

DOI: 10.1021/acs.inorgchem.5b00921
Inorg. Chem. 2015, 54, 6958−6967

Table 4. Electrochemical and ECL Data

	ACN				H_2O	
sample	$E_{1/2}{}^{a}$ (Ir^{3+}/Ir^{4+}) (V)	$E_{red}{}^{a}$ (phen/phen$^-$) (V)	$E_{1/2}{}^{a}$ (ppy/ppy$^-$) (V)	ECL[b]	$E_{p,ox}{}^{a}$	ECL[b,c]
1	1.33	−1.57	−2.18	1.00	1.39	1.00
2	1.38	−1.62	−2.08	0.44	1.18	0.79
3	1.34	−1.60	−2.23	1.11	1.44	
4	1.27	−1.62	−2.23	0.71	1.25	
5	1.30	−1.54	−2.13	2.07	1.23	0.57
6	1.24	−1.62	−2.23	0.73	1.23	
7	1.26	−1.44	−2.09	4.26[d]	1.05	4.46

[a]Potentials are given vs the Ag/AgCl quasireference electrode. The $E_{1/2}$ for ferrocene methanol added as an internal standard is 0.48 V.[75] [b]Normalized to complex **1**. [c][Iridium] = 0.05 mM for buffered solutions. [d]The intensity of complex **7** was not stable over continuous CV cycles.

electron oxidation peak around $E_{1/2}$ = 1.3 V (vs Ag/AgCl-QRE) and a one-electron reduction peak around $E_{1/2}$ = −1.6 V (vs Ag/AgCl-QRE) (Figure 6a).[68] The quasireversible oxidation peak is assigned to the $Ir^{3+/4+}$ couple. Furthermore, changing the scan rate (50−600 mV/s) still resulted in quasireversible behavior. The close correspondence of the $E_{1/2}$ for $Ir^{3+/4+}$ for all complexes **1**−**6** (Table 4) suggests that the HOMO of the Ir^{3+} center is not greatly perturbed by the substitution of the imidazole phenanthroline portion of the complexes. This is consistent with a HOMO that is centered on the metal and the 2-phenylpyridinato ligands.[69] The 3+ and 4+ forms are stable over repeated CV scans. The anodic and cathodic peak currents (i_{pa} and i_{pc1}, respectively) were proportional to the square root of the scan rate ($v^{1/2}$) (Supporting Information Figure S11). From the slope of i_{pa} versus $v^{1/2}$ plot, the Randles−Sevcik equation yielded a diffusion coefficient of 2.43 × 10^{-5} cm^2/s for complex **5**, and the other complexes can be expected to have similar values.

The reversible reduction peak at around $E_{1/2}$ of −0.8 V is assigned to a TBA^+ stabilized O_2 reduction[70,71] (Supporting Information Figure S12), and as such presents no significant shift with the various iridium complexes. The irreversible reduction peak in the range −1.54 to −1.62 V is assigned to the phenanthroline ligands, which is consistent with the assignment of the unmodified phenanthroline ligand in complex **7** (−1.44 V).[72] Finally, the reduction of the 2-phenylpyridinato ligands is visible for most complexes at around −2.2 V.[73] These assignments are based on literature precedents.

The CVs of iridium complexes (0.05 mM) were also recorded in aqueous buffer solution (0.2 M Tris, pH 7.4) (Figure 6b). Under these conditions, the oxidation waves were broader than those in acetonitrile and were irreversible, and thus in Table 4 the oxidation peak potential ($E_{p,ox}$) is reported. With the exception of **1** and **3**, most complexes showed similar oxidation peaks ($E_{p,ox}$ = ∼1.2−1.5 V). Compared to their oxidation in acetonitrile, all complexes except **1** and **3** were

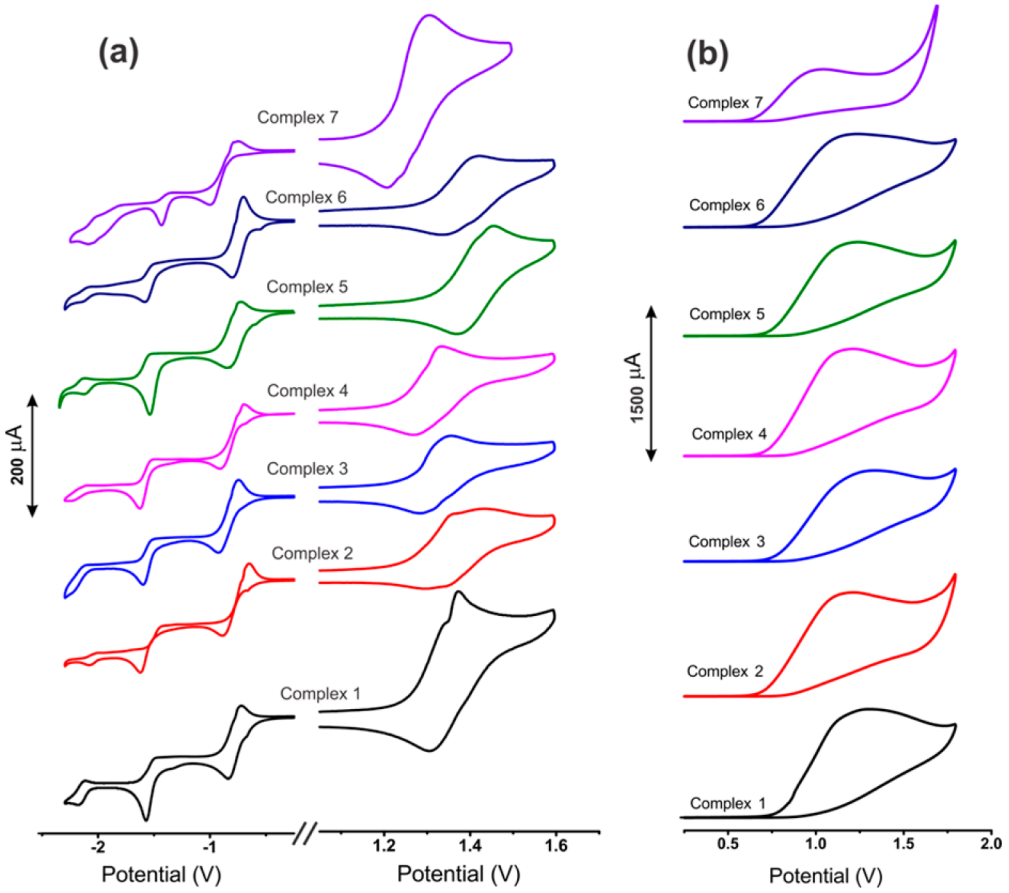

Figure 6. CV results for complexes **1**−**7**: (a) in acetonitrile solution, and (b) in aqueous buffer solution. The test solutions contained 0.5 mM iridium complex and 0.1 M $TBAPF_6$ (acetonitrile) or 0.05 mM iridium complex and 0.2 M Tris buffer, pH 7.4 (aqueous). The potential was cycled between −2.25 and 1.65 V (acetonitrile), or between −0.45 and 1.75 V (buffer) at a scan rate of 100 mV/s.

DOI: 10.1021/acs.inorgchem.5b00921
Inorg. Chem. 2015, 54, 6958−6967

oxidized at less anodic potentials in buffer solutions, consistent with the increased polarity of the medium facilitating the $Ir^{3+/4+}$ oxidation.[74] The oxidation peaks of **1** and **3** in buffer are slightly more anodic than the other samples. Interestingly, there were no observed reduction peaks in the buffered solution.

The ECL of the complexes was examined through the co-reactant mechanism. This relies on the oxidation of tri(n-propyl)amine (TPrA), which yields a strong reducing agent ($TPrA^{\bullet}$) that reacts with the oxidized iridium complexes to generate an excited state.[25,68,76−79] This mechanism can occur both in organic and aqueous solvents, allowing comparison of ECL behavior in these two media. In acetonitrile and in the presence of 0.05 M TPrA, the ECL was measured during multiple continuous CV scans, and the average integrated intensity, relative to **1**, is listed in Table 4. The ECL was observed during the forward potential scan between 1.0 and 2.0 V, with a maximum intensity at approximately 1.5 V (Figure 7a). The ECL spectra are shown in Figure 7b and overlap well

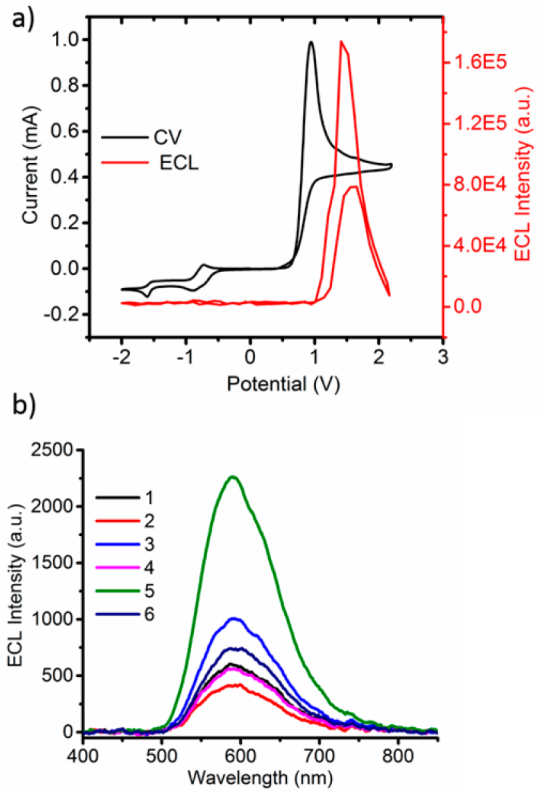

Figure 7. (a) Overlay of the simultaneous CV (black) and ECL (red) scans for complex **5**; (b) ECL spectra of **1**−**6**. Both experiments are in MeCN with [iridium complex] = 0.5 mM, [$TBAPF_6$] = 0.1 M, and [TPrA] = 0.05 M.

with the fluorescence spectra indicating that similar excited states are involved for both processes.[74,80] At potentials more anodic than +1.5 V, ECL is decreased possibly as a result of quenching by the TPrA radical cation formed at higher oxidation potentials.[81] The reduced ECL response persists during the reverse scan. For complexes **1**−**6**, the ECL intensity remained consistent over the multiple continuous CV cycles. The stability of the ECL response is noteworthy.[82] In comparison, under identical conditions, the unsubstituted **7** had a stronger (~2.5 times) ECL intensity during the first CV scan, but it drastically decreased with subsequent CV scans (Supporting Information Figure S13). The electrogenerated Ir excited state in the ECL experiment partly arises from the combination of tripropylamine radicals ($TPrA^{\bullet}$) with the oxidized metal complex ($Ir^{+\bullet}$ + $TPrA^{\bullet}$ → Ir* + TPrA side product). The efficiency of ECL thus depends on the energy match between the HOMO of $TPrA^{\bullet}$ and the LUMO of the oxidized metal complex.[83] The higher ECL intensity of phen complex **7** compared to those of **1**−**6** may be related to the less electron-rich (lower LUMO energy) phenanthroline ligand in **7** compared to the imidazole phenanthroline ligand in **1**−**6**.[84] The reason for the observed robustness of the ECL signal for complexes **1**−**6** is unclear at present, but may possibly be related to increased stabilization of the complex against degradation, imparted by the extended imidazole phenanthroline ligand compared to the phenanthroline. The increased stability of the ECL signals for **1**−**6** allows the collection of more photons upon repeated ECL scans, thus increasing sensitivity.

Interestingly as well, the ECL intensities increased with increasing electron withdrawing ability of the phenyl group attached to the imidazole phenanthroline ligand. In fact, they correlated well with Hammett σ values of the substituents on the phenyl group of the imidazole phenanthroline moiety[85] (Supporting Information Figure S14). We are currently investigating this trend, specifically regarding the extent of delocalization between the imidazole−phenanthroline ligand and the attached phenyl group.[12,84,86] From the complexes examined here, *o*-chloro complex **5** and trifluoromethyl complex **3** had the most intense ECL response (the ECL intensity of **5** is twice that of **1**).

To use iridium complexes in subsequent G-quadruplex binding experiments, ECL measurements of selected iridium complexes were also conducted in aqueous buffer solutions (Table 4). All samples were less emissive compared to the ECL in acetonitrile solution, and the difference between their ECL intensities was less pronounced. This reduction in ECL emissivity mirrors the decreased photoluminescence intensities observed above.

ECL-Based DNA Detection. Since these complexes bind selectively to G-quadruplex sequences, we examined whether this binding may also affect their ECL response, potentially leading to an interesting detection method. In preliminary experiments, the ECL response of three complexes **1**, **2**, and **5** in buffer (with added TPrA) was measured in the absence and presence of the G-quadruplex sequence c-myc (ratios of Ir/DNA were varied from 500 to 36) (Figure 8). These complexes were selected on the basis of their ECL responses in acetonitrile; **1** is the parent complex, and **2** and **5** produce the smallest and largest ECL responses, respectively. Interestingly, as the c-myc DNA content of the solutions is increased, the ECL response increases. It reaches a maximum value at (Ir:DNA quadruplex = 167:1), and decreases at higher DNA concentrations. Many biological assays involve samples with very small analyte concentrations, and this ECL range is suitable for these assays. This response was reproduced for all three tested complexes, which showed similar intensity with added c-myc (Figure 8a).

To confirm that the complex:DNA interaction is specific to the G-quadruplex sequence, we conducted two experiments under the same conditions. First, we tested phenyl complex **1** (Figure 8b) in the presence of duplex DNA and both G-quadruplex sequences c-myc and 22AG-K, at the same concentration as the experiment above (concentration in

DOI: 10.1021/acs.inorgchem.5b00921
Inorg. Chem. 2015, 54, 6958−6967

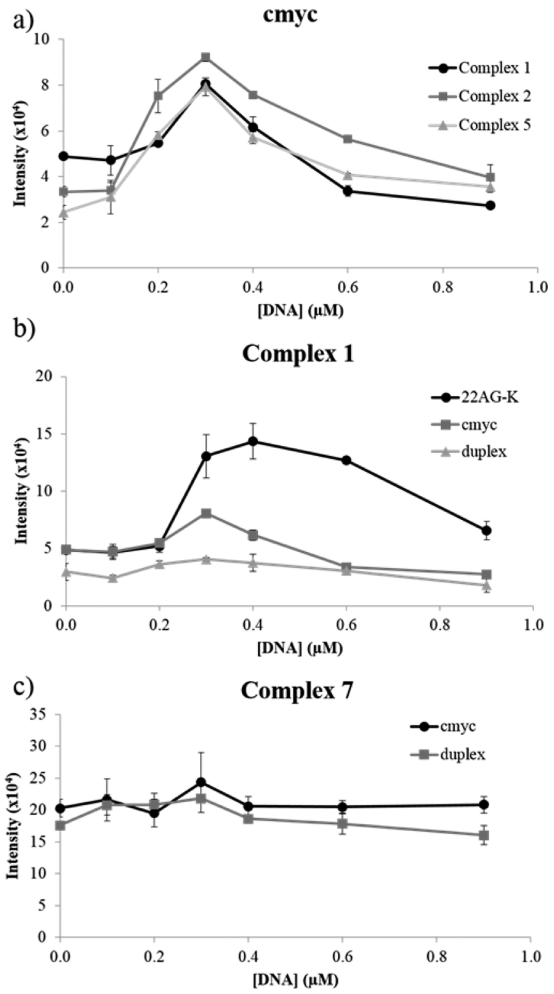

Figure 8. ECL response as a function of added DNA: (a) ECL intensity of **1**, **2**, and **5** as c-myc G-quadruplex is added; (b) ECL of **1** with added c-myc and 22AG-K G-quadruplex sequences and duplex DNA; (c) ECL of control complex **7** with c-myc and duplex DNA.

structure, that is, one quadruplex and one duplex). The results show that the addition of duplex DNA has a smaller effect on the ECL intensity than does the c-myc G-quadruplex sequence. Interestingly, the addition of 22AG-K causes a marked increase of the ECL intensity. The second experiment was conducted using **7** (Figure 8c) which should not show preference for G-quadruplex sequences over duplex DNA. In these experiments we added either c-myc or duplex DNA to solutions of **7** and saw minimal changes in the ECL intensity as the DNA content was increased. These experiments suggest that **1**, **2**, and **5** interact specifically with G-quadruplex sequences and can detect their presence as low as 0.1 μM (using our ECL setup) based on ECL response. Thus, while the original ECL intensity of **7** is higher than those of complexes **1**, **2**, and **5**, complex **7** does not show a response in the presence of G-quadruplexes, and its ECL is not robust through many cycles.

The observed ECL enhancement of complexes **1**, **2**, and **5** may be related to the light-switch effect noted for photoluminescence experiments, in which the environment of the complex while π-stacked on the G-quadruplex results in enhanced emission. In fact, the greater ECL increase for **1** upon addition of 22AG-K compared to c-myc parallels its photoluminescence behavior with 22AG-K and c-myc (Table 2). This phenomenon is structure-specific, as duplex DNA does not cause this ECL enhancement and different quadruplex structures cause different ECL responses. Moreover, complex **7**, which does not end-stack onto guanine quadruplexes but likely interacts via groove binding with DNA, did not show an ECL increase with these structures.

As hypothesized above, the binding site of the G-quadruplexes, particularly the 22AG-K polymorph, may effectively shield the complex from the solvent and result in enhanced ECL. In addition, as DNA is negatively charged, it may bring the iridium complexes and the co-reactant (TPrA, which is expected to be protonated) in close proximity for an efficient bimolecular reaction to generate the iridium excited state. However, at higher DNA concentration, association of complexes may possibly occur, resulting in gradual loss of the ECL signal. It is important to note here that the range of ECL increase (up to 167:1 Ir:DNA) is useful, in that it allows the detection of small amounts of guanine quadruplexes.[87] These experiments, while demonstrating the exciting potential of these complexes as ECL-based G-quadruplex indicators, are preliminary. We are currently examining this phenomenon further to determine the precise mechanism by which this enhancement occurs, and to measure and improve its dynamic range and DNA detection limit.

CONCLUSIONS

In conclusion, we have described six iridium complexes with extended imidazole phenanthroline ancillary ligands and assessed their binding ability with various forms of biologically relevant DNA sequences, including G-quadruplexes from human telomeric and oncogene promoter sequences as well as duplex DNA. These complexes exhibit luminescence enhancement upon binding specifically to G-quadruplex DNA, but not to duplex or single-stranded DNA. We showed the use of these complexes as selective luminescent dyes for detection of G-quadruplexes in agarose gel electrophoresis. They were able to discriminate between G-quadruplex structures and double-stranded DNA, but also among different G-quadruplex polymorphs found in biologically relevant structures. These complexes exhibit electrogenerated chemiluminescence (ECL) in organic solvents. In aqueous solvent, the ECL signal significantly increased upon addition of guanine quadruplexes, but not duplex DNA. This phenomenon is also selective between different G-quadruplex structures. The promising results from this preliminary assay may allow the direct detection of low levels of G-quadruplex DNA in a selective manner in aqueous conditions.

ASSOCIATED CONTENT

Supporting Information

Experimental materials, instrumentation, and methods; synthetic details and characterization (including ^{1}H and ^{13}C NMR) for complexes **1**−**6**; DNA sequences, preparation, and handling procedures; X-ray crystallography data; absorbance and luminescence spectra of **1**−**6** in DCM and water; luminescence spectra of **1**−**6** with added ssDNA; luminescence of **7** with added DNA; CD spectra of G-quadruplex DNA with added **1** and **7**; binding curves for **1**−**6** with 22AG-K and cmyc; thermal denaturation of dsDNA with and without **1**; agarose gel images from staining assay and gel emission intensity graphs for complexes **1**−**5** vs SYBR gold; i_{pa} vs $v^{1/2}$ for **5**; CV of $TBAPF_6$ blank solution; integrated emission intensities of **1** and **7** over 5 continuous CV cycles; ECL intensities; and Hammett plot for **1**−**6**. The Supporting Information is available free of charge on

DOI: 10.1021/acs.inorgchem.5b00921
Inorg. Chem. 2015, 54, 6958−6967

the ACS Publications website at DOI: 10.1021/acs.inorgchem.5b00921.

AUTHOR INFORMATION

Corresponding Authors

*E-mail: janine.mauzeroll@mcgill.ca.
*E-mail: hanadi.sleiman@mcgill.ca.

Notes

The authors declare no competing financial interest.

ACKNOWLEDGMENTS

The authors thank NSERC (H.F.S., J.M.), CFI (H.F.S., J.M.), CSACS (H.F.S., J.M.), and the Canada Research Chairs program (H.F.S.) for financial support. H.F.S. is a Cottrell Scholar of the Research Corporation.

REFERENCES

(1) De Cian, A.; Lacroix, L.; Douarre, C.; Temime-Smaali, N.; Trentesaux, C.; Riou, J.-F.; Mergny, J.-L. *Biochimie* **2008**, *90*, 131.
(2) Brooks, T. A.; Kendrick, S.; Hurley, L. *FEBS J.* **2010**, *277*, 3459.
(3) Murat, P.; Balasubramanian, S. *Curr. Opin. Genet. Dev.* **2014**, *25*, 22.
(4) Deng, M.; Zhang, D.; Zhou, Y.; Zhou, X. *J. Am. Chem. Soc.* **2008**, *130*, 13095.
(5) Du, Y.; Li, B.; Wang, E. *Acc. Chem. Res.* **2013**, *46*, 203.
(6) Roembke, B. T.; Nakayama, S.; Sintim, H. O. *Methods* **2013**, *64*, 185.
(7) Shen, J.; Li, Y.; Gu, H.; Xia, F.; Zuo, X. *Chem. Rev.* **2014**, *114*, 7631.
(8) Monchaud, D.; Teulade-Fichou, M.-P. *Org. Biomol. Chem.* **2008**, *6*, 627.
(9) Georgiades, S. N.; Abd Karim, N. H.; Suntharalingam, K.; Vilar, R. *Angew. Chem., Int. Ed.* **2010**, *49*, 4020.
(10) Biver, T. *Coord. Chem. Rev.* **2013**, *257*, 2765.
(11) Kieltyka, R.; Englebienne, P.; Fakhoury, J.; Autexier, C.; Moitessier, N.; Sleiman, H. F. *J. Am. Chem. Soc.* **2008**, *130*, 10040.
(12) Castor, K. J.; Mancini, J.; Fakhoury, J.; Weill, N.; Kieltyka, R.; Englebienne, P.; Avakyan, N.; Mittermaier, A.; Autexier, C.; Moitessier, N.; Sleiman, H. F. *ChemMedChem* **2012**, *7*, 85.
(13) Castor, K. J.; Liu, Z.; Fakhoury, J.; Hancock, M. A.; Mittermaier, A.; Moitessier, N.; Sleiman, H. F. *Chem.—Eur. J.* **2013**, *19*, 17836.
(14) Rickling, S.; Ghisdavu, L.; Pierard, F.; Gerbaux, P.; Surin, M.; Murat, P.; Defrancq, E.; Moucheron, C.; Kirsch-De Mesmaeker, A. *Chem.—Eur. J.* **2010**, *16*, 3951.
(15) Wilson, T.; Williamson, M. P.; Thomas, J. A. *Org. Biomol. Chem.* **2010**, *8*, 2617.
(16) Largy, E.; Hamon, F.; Rosu, F.; Gabelica, V.; De Pauw, E.; Guedin, A.; Mergny, J.-L.; Teulade-Fichou, M.-P. *Chem.—Eur. J.* **2011**, *17*, 13274.
(17) Manet, I.; Manoli, F.; Donzello, M. P.; Viola, E.; Andreano, G.; Masi, A.; Cellai, L.; Monti, S. *Org. Biomol. Chem.* **2011**, *9*, 684.
(18) Yao, J.-L.; Gao, X.; Sun, W.; Fan, X.-Z.; Shi, S.; Yao, T.-M. *Inorg. Chem.* **2012**, *51*, 12591.
(19) Leung, C. H.; Zhong, H. J.; Chan, D. S. H.; Ma, D. L. *Coord. Chem. Rev.* **2013**, *257*, 1764.
(20) Leung, C. H.; Zhong, H. J.; Yang, H.; Cheng, Z.; Chan, D. S. H.; Ma, V. P. Y.; Abagyan, R.; Wong, C. Y.; Ma, D. L. *Angew. Chem., Int. Ed.* **2012**, *51*, 9010.
(21) Ma, D. L.; Chan, D. S. H.; Leung, C. H. *Acc. Chem. Res.* **2014**, *47*, 3614.
(22) Man, B. Y. W.; Chan, H. M.; Leung, C. H.; Chan, D. S. H.; Bai, L. P.; Jiang, Z. H.; Li, H. W.; Ma, D. L. *Chem. Sci.* **2011**, *2*, 917.
(23) Jacques, A.; Kirsch-De Mesmaeker, A.; Elias, B. *Inorg. Chem.* **2014**, *53*, 1507.
(24) Lo, K. K. W.; Li, S. P. Y.; Zhang, K. Y. *New J. Chem.* **2011**, *35*, 265.
(25) Miao, W. *Chem. Rev.* **2008**, *108*, 2506.
(26) You, Y. *Curr. Opin. Chem. Biol.* **2013**, *17*, 699.
(27) Lo, K. K.-W.; Chung, C.-K.; Zhu, N. *Chem.—Eur. J.* **2006**, *12*, 1500.
(28) Lepeltier, M.; Lee, T. K.-M.; Lo, K. K.-W.; Toupet, L.; Le Bozec, H.; Guerchais, V. *Eur. J. Inorg. Chem.* **2005**, 110.
(29) Li, C.; Lin, J.; Guo, Y.; Zhang, S. *Chem. Commun.* **2011**, *47*, 4442.
(30) Li, M.-J.; Jiao, P.; Lin, M.; He, W.; Chen, G.-N.; Chen, X. *Analyst* **2011**, *136*, 205.
(31) Leung, K. H.; He, H. Z.; He, B. Y.; Zhong, H. J.; Lin, S.; Wang, Y. T.; Ma, D. L.; Leung, C. H. *Chem. Sci.* **2015**, *6*, 2166.
(32) Leung, K. H.; He, H. Z.; Ma, V. P. Y.; Zhong, H. J.; Chan, D. S. H.; Zhou, J.; Mergny, J. L.; Leung, C. H.; Ma, D. L. *Chem. Commun.* **2013**, *49*, 5630.
(33) Lu, L. H.; Chan, D. S. H.; Kwong, D. W. J.; He, H. Z.; Leung, C. H.; Ma, D. L. *Chem. Sci.* **2014**, *5*, 4561.
(34) Zhao, Q.; Liu, S.; Shi, M.; Li, F.; Jing, H.; Yi, T.; Huang, C. *Organometallics* **2007**, *26*, 5922.
(35) Dragonetti, C.; Falciola, L.; Mussini, P.; Righetto, S.; Roberto, D.; Ugo, R.; Valore, A.; De Angelis, F.; Fantacci, S.; Sgamellotti, A.; Ramon, M.; Muccini, M. *Inorg. Chem.* **2007**, *46*, 8533.
(36) Juris, A.; Balzani, V.; Barigelletti, F.; Campagna, S.; Belser, P.; Von Zelewsky, A. *Coord. Chem. Rev.* **1988**, *84*, 85.
(37) Kiran, R. V.; Hogan, C. F.; James, B. D.; Wilson, D. J. D. *Eur. J. Inorg. Chem.* **2011**, *2011*, 4816.
(38) Neve, F.; La Deda, M.; Crispini, A.; Bellusci, A.; Puntoriero, F.; Campagna, S. *Organometallics* **2004**, *23*, 5856.
(39) Yang, H.; Ma, V. P. Y.; Chan, D. S. H.; He, H. Z.; Leung, C. H.; Ma, D. L. *Curr. Med. Chem.* **2013**, *20*, 576.
(40) Zhao, Q.; Liu, S.; Shi, M.; Wang, C.; Yu, M.; Li, L.; Li, F.; Yi, T.; Huang, C. *Inorg. Chem.* **2006**, *45*, 6152.
(41) Lowry, M. S.; Hudson, W. R.; Pascal, R. A., Jr.; Bernhard, S. *J. Am. Chem. Soc.* **2004**, *126*, 14129.
(42) Wilde, A. P.; King, K. A.; Watts, R. J. *J. Phys. Chem.* **1991**, *95*, 629.
(43) Colombo, M. G.; Hauser, A.; Guedel, H. U. *Inorg. Chem.* **1993**, *32*, 3088.
(44) Colombo, M. G.; Guedel, H. U. *Inorg. Chem.* **1993**, *32*, 3081.
(45) The DCM solutions were not stringently degassed.
(46) Hackett, J. W., II; Turro, C. *J. Phys. Chem. A* **1998**, *102*, 5728.
(47) Oddy, F. E.; Brovelli, S.; Stone, M. T.; Klotz, E. J. F.; Cacialli, F.; Anderson, H. L. *J. Mater. Chem.* **2009**, *19*, 2846.
(48) Kieltyka, R.; Fakhoury, J.; Moitessier, N.; Sleiman, H. F. *Chem.—Eur. J.* **2008**, *14*, 1145.
(49) Friedman, A. E.; Chambron, J. C.; Sauvage, J. P.; Turro, N. J.; Barton, J. K. *J. Am. Chem. Soc.* **1990**, *112*, 4960.
(50) Sabatani, E.; Nikol, H. D.; Gray, H. B.; Anson, F. C. *J. Am. Chem. Soc.* **1996**, *118*, 1158.
(51) Olson, E. J. C.; Hu, D.; Hoermann, A.; Jonkman, A. M.; Arkin, M. R.; Stemp, E. D. A.; Barton, J. K.; Barbara, P. F. *J. Am. Chem. Soc.* **1997**, *119*, 11458.
(52) Onfelt, B.; Lincoln, P.; Norden, B.; Baskin, J. S.; Zewail, A. H. *Proc. Natl. Acad. Sci. U.S.A.* **2000**, *97*, 5708.
(53) Pedras, B.; Batista, R. M. F.; Tormo, L.; Costa, S. P. G.; Raposo, M. M. M.; Orellana, G.; Capelo, J. L.; Lodeiro, C. *Inorg. Chim. Acta* **2012**, *381*, 95.
(54) Stephenson, M.; Reichardt, C.; Pinto, M.; Wachtler, M.; Sainuddin, T.; Shi, G.; Yin, H.; Monro, S.; Sampson, E.; Dietzek, B.; McFarland, S. A. *J. Phys. Chem. A* **2014**, *118*, 10507.
(55) Luu, K. N.; Phan, A. T.; Kuryavyi, V.; Lacroix, L.; Patel, D. J. *J. Am. Chem. Soc.* **2006**, *128*, 9963.
(56) Ambrus, A.; Chen, D.; Dai, J.; Jones, R. A.; Yang, D. *Biochemistry* **2005**, *44*, 2048.
(57) Gabelica, V.; Baker, E. S.; Teulade-Fichou, M.-P.; De Pauw, E.; Bowers, M. T. *J. Am. Chem. Soc.* **2007**, *129*, 895.
(58) Le, H. T.; Miller, M. C.; Buscaglia, R.; Dean, W. L.; Holt, P. A.; Chaires, J. B.; Trent, J. O. *Org. Biomol Chem.* **2012**, *10*, 9393.
(59) Siddiqui-Jain, A.; Grand, C. L.; Bearss, D. J.; Hurley, L. H. *Proc. Natl. Acad. Sci. U.S.A.* **2002**, *99*, 11593.

DOI: 10.1021/acs.inorgchem.5b00921
Inorg. Chem. 2015, 54, 6958−6967

(60) Wu, P.; Ma, D.-L.; Leung, C.-H.; Yan, S.-C.; Zhu, N.; Abagyan, R.; Che, C.-M. *Chem.—Eur. J.* **2009**, *15*, 13008.
(61) Agarwal, T.; Roy, S.; Chakraborty, T. K.; Maiti, S. *Biochemistry* **2010**, *49*, 8388.
(62) Shalaby, T.; von Bueren, A. O.; Huerlimann, M.-L.; Fiaschetti, G.; Castelletti, D.; Masayuki, T.; Nagasawa, K.; Arcaro, A.; Jelesarov, I.; Shin-ya, K.; Grotzer, M. *Mol. Cancer Ther.* **2010**, *9*, 167.
(63) Wang, P.; Leung, C.-H.; Ma, D.-L.; Yan, S.-C.; Che, C.-M. *Chem.—Eur. J.* **2010**, *16*, 6900.
(64) Ou, T.-M.; Lin, J.; Lu, Y.-J.; Hou, J.-Q.; Tan, J.-H.; Chen, S.-H.; Li, Z.; Li, Y.-P.; Li, D.; Gu, L.-Q.; Huang, Z.-S. *J. Med. Chem.* **2011**, *54*, 5671.
(65) Our previous results described in Castor, K. J.; Liu, Z.; Fakhoury, J.; Hancock, M. A.; Mittermaier, A.; Moitessier, N.; Sleiman, H. F. *Chem.—Eur. J.* **2013**, *19*, 17836 showed that c-myc and 22AG-K are very stable under our experimental conditions, and have high melting temperatures such that melting is not observed. If salt is removed the melting temperatures are decreased, as is the CD signal, suggesting that under such conditions the G-quadruplexes may not be fully folded..
(66) Largy, E.; Hamon, F.; Teulade-Fichou, M.-P. *Anal. Bioanal. Chem.* **2011**, *400*, 3419.
(67) Greschner, A. A.; Bujold, K. E.; Sleiman, H. F. *J. Am. Chem. Soc.* **2013**, *135*, 11283.
(68) Tefashe, U. M.; Metera, K. L.; Sleiman, H. F.; Mauzeroll, J. *Langmuir* **2013**, *29*, 12866.
(69) Zhu, S.; Song, Q.; Zhang, S.; Ding, Y. *J. Mol. Struct.* **2013**, *1035*, 224.
(70) Laoire, C. O.; Mukerjee, S.; Abraham, K. M.; Plichta, E. J.; Hendrickson, M. A. *J. Phys. Chem. C* **2010**, *114*, 9178.
(71) Laoire, C. O.; Mukerjee, S.; Abraham, K. M.; Plichta, E. J.; Hendrickson, M. A. *J. Phys. Chem. C* **2009**, *113*, 20127.
(72) Goldsmith, J. I.; Hudson, W. R.; Lowry, M. S.; Anderson, T. H.; Bernhard, S. *J. Am. Chem. Soc.* **2005**, *127*, 7502.
(73) Zhao, H.-D.; Zhu, X.-G.; Zhang, Y.-M. *J. Appl. Phys.* **2002**, *92*, 1.
(74) Bruce, D.; Richter, M. M. *Anal. Chem.* **2002**, *74*, 1340.
(75) Gagne, R. R.; Koval, C. A.; Lisensky, G. C. *Inorg. Chem.* **1980**, *19*, 2854.
(76) Richter, M. M. *Chem. Rev.* **2004**, *104*, 3003.
(77) Bandini, M.; Bianchi, M.; Valenti, G.; Piccinelli, F.; Paolucci, F.; Monari, M.; Umani-Ronchi, A.; Marcaccio, M. *Inorg. Chem.* **2010**, *49*, 1439.
(78) Shu, Q. H.; Birlenbach, L.; Schmittel, M. *Inorg. Chem.* **2012**, *51*, 13123.
(79) Swanick, K. N.; Ladouceur, S.; Zysman-Colman, E.; Ding, Z. F. *Chem. Commun.* **2012**, *48*, 3179.
(80) Yu, L.; Huang, Z.; Liu, Y.; Zhou, M. *J. Organomet. Chem.* **2012**, *718*, 14.
(81) Doeven, E. H.; Zammit, E. M.; Barbante, G. J.; Francis, P. S.; Barnett, N. W.; Hogan, C. F. *Chem. Sci.* **2013**, *4*, 977.
(82) Lai, R. Y.; Bard, A. J. *J. Phys. Chem. B* **2003**, *107*, 5036.
(83) Stringer, B. D.; Quan, L. M.; Barnard, P. J.; Wilson, D. J. D.; Hogan, C. F. *Organometallics* **2014**, *33*, 4860.
(84) Kim, J. I.; Shin, I.-S.; Kim, H.; Lee, J.-K. *J. Am. Chem. Soc.* **2005**, *127*, 1614.
(85) Hansch, C.; Leo, A.; Taft, R. W. *Chem. Rev.* **1991**, *91*, 165.
(86) Betteridge, P. W.; Carruthers, J. R.; Cooper, R. I.; Prout, K.; Watkin, D. J. *J. Appl. Crystallogr.* **2003**, *36*, 1487.
(87) Hu, L.; Bian, Z.; Li, H.; Han, S.; Yuan, Y.; Gao, L.; Xu, G. *Anal. Chem.* **2009**, *81*, 9807.

DOI: 10.1021/acs.inorgchem.5b00921
Inorg. Chem. 2015, 54, 6958−6967